Development 127, 1509-1516 (2000)
Printed in Great Britain © The Company of Biologists Limited 2000
DEV1516

Local, possibly contact-mediated signalling restricted to homotypic neurons controls the regular spacing of cells within the cholinergic arrays in the developing rodent retina

Lucia Galli-Resta

Istituto di Neurofisiologia CNR, via Alfieri 1, 56017 Ghezzano (Pi), Italy
e-mail: galli@in.pi.cnr.it

Accepted 21 January; published on WWW 7 March 2000

SUMMARY

In the vertebrate retina neurons of the same type commonly form non-random arrays, assembled by unknown positional mechanisms during development. Computational models in which no two cells are closer than a minimal distance, simulate many retinal arrays. These findings have important biological implications, since they suggest that cells are determined as neurons of specific types before entering their arrays, and that local, possibly contact-mediated interactions acting exclusively among the elements of an array account for its assembly. This is here verified by combining experimental manipulations in normal and transgenic models with computational analysis for the cholinergic mosaics, the only arrays so far for which the development of spatial ordering is known quantitatively. When generalised, these findings suggest a plan for vertebrate retinal patterning, where homotypic interactions organise retinal arrays first, then local interactions between synaptic partners suffice to establish the topographical connections that support retinal processing.

Key words: Patterning, Retinal mosaics, Acetylcholine, Rat

INTRODUCTION

The vertebrate retina exemplifies a modular circuitry typical of many regions of the central nervous system, where a limited number of principal types of neurons are regularly arranged in layers. Decades of morphological, physiological and biochemical studies have lead to the characterisation of many different cell subtypes within each principal class of retinal neurons (Dowling, 1987; Wässle and Boycott, 1991; Rodieck, 1998). This analysis has also revealed a fundamental principle of retinal organisation, as the majority of neuronal types are spaced in an orderly manner within their layer, forming arrays of homotypic neurons that regularly tile the retina (Wässle and Riemann, 1978; Wässle and Boycott, 1991; MacNeil and Masland, 1998; Rodieck, 1998; Cook and Chalupa, 2000). This modular organisation confers on the retina an enormous power of parallel processing (Wässle and Boycott, 1991; Masland, 1996), yet little is known of the way retinal arrays, or mosaics, form during development (Galli-Resta, 1998; Cook and Chalupa, 2000).

The retina originates from a proliferative tissue where cell divisions occur in the innermost region, and neurons then migrate to their final destinations. Until recently, the lack of markers expressed early in development prevented the analysis of mosaic formation. However, as new markers became available, specific retinal mosaics could be studied at some stages in their development, and these included mosaics of photoreceptors, horizontal and amacrine cells. The general picture that has emerged is that arrays are regular before all their elements have been generated, or before these have reached the mosaic layers. This is true in fish, birds and mammals and indicates that forming regular arrays is an early constraint on mosaic neurons (Larison and Bremiller, 1990; Wikler and Rakic, 1991; Raymond et al., 1995; Cepko, 1996; Bumsted et al., 1997; Wikler et al., 1997). A direct consequence of early mosaic formation is a limit to the number of cells of the same type that can settle in a given region. This may be achieved by controls on cell genesis or cell fate determination, by influencing the trajectory of cell migration, or by making cell death depend on the cell position within the array (Galli-Resta, 1998). Thus, the biological mechanisms leading to array formation act at the core of tissue development and patterning.

Among the earliest detectable arrays are those formed by the cholinergic amacrine cells which play an essential role in the propagation of the early spontaneous activity that shapes the visual circuitry (Feller et al., 1996; Penn et al., 1998). The two cholinergic arrays are regular when they still do not contain all their elements, and newly arriving cells preserve the geometry of the array (Galli-Resta et al., 1997). Computational analysis has shown that cell distributions where no two cell bodies are closer than a fixed minimal distance are geometrically indistinguishable from the developing cholinergic mosaics (Galli-Resta et al., 1997; Galli-Resta, 1998). Thus, arrays could

form if each cell is able to exclude cells of like type from a limited domain surrounding it. A similar rule is also sufficient to explain the organisation of the immature horizontal cell mosaic (Scheibe et al., 1995) and that of adult photoreceptor mosaics (Galli-Resta et al., 1999). These findings have important biological implications, since they suggest that cells are determined as neurons of specific types before entering their arrays, and that local interactions acting exclusively among the elements of an array account for its assembly. These issues have been tested experimentally for the cholinergic arrays, the only arrays so far for which the development of spatial ordering has been described quantitatively (Galli-Resta et al., 1997; Galli-Resta, 1998; Cook and Chalupa, 2000). In the experiments described here, I have searched for indicators of cholinergic cell differentiation prior to cell entry into the arrays, finding that two markers unique to cholinergic cells are expressed by cells that are still outside the array layers. To test whether the interactions that regularly space the elements of the cholinergic arrays are independent of other cell types, I have analysed the spatial organisation of the arrays when the numerical ratio of the cholinergic cells and their synaptic/neighbouring cell types is altered, either by means of experimental manipulations or in a transgenic model. Finally, I have analysed by means of autocorrelation techniques the spatial range and the lack of additivity of the interactions that regularly space the elements of the cholinergic arrays.

MATERIALS AND METHODS

Experiments in compliance with the national regulation and the ARVO statement on animal experimentation were performed on Long Evan hooded rats, C57 bl/6 mice (wild type) and transgenic mice from the NSE73a line overexpressing human BCL2 under the control of neuron-specific enolase (Dubois-Dauphin et al., 1994; Cenni et al., 1996). The presence of the *BCL2* transgene was assessed by polymerase chain reaction on DNA extracted from the tail tissue of the mice. Intracranial optic nerve section in neonatal rats was performed under anaesthesia as described by Perry et al. (1983). Eye collection, dissection, fixation, mounting and immunostaining were performed as described by Galli-Resta and Ensini (1996); Galli-Resta et al. (1997). Cholinergic cells were identified by means of polyclonal antibodies to ChAT or VAChT (Chemicon), or a monoclonal antibody to Islet1 (gift of T. Jessel, Columbia University).

Data acquisition

Samples of both ChAT arrays were taken at regularly spaced locations going from the centre to the periphery in 4 orthogonal directions (or more) in whole-mounted retinas, using a Leica TCNS confocal microscope. Retinas were drawn before and after reaction, and after analysis to control for tissue shrinkage/compression. Sampled fields and retinal drawings were fed to an Image analyser (Imaging Ontario, Canada) to obtain cell density, cell positioning and retinal area. The total number of cells was determined as the average density times the retinal area. Three normal rat retina and three retinas after optic nerve section at birth were analysed on postnatal day 3 (P3), and the same number of cases were compared on P12. At both ages 400×400 μm^2 sampling fields were analysed. The analysis of cell pairs was performed on 6 P4 normal rat retinas in sampling fields of 400×400 μm^2. The mouse data are derived from 3 wild-type and 3 BCL2 adult mice (sampling fields 250×250 μm^2). Between 1/20 and 1/5 of each retina were sampled in all cases. Whole mounts and 300-500 μm thick cross sections of embryonic and neonatal retinas were analysed to determine whether specific cholinergic markers are expressed by cells which are still outside the cholinergic arrays.

Spatial data analysis

Nearest neighbour distances, Voronoi and Delaunay tessellation, autocorrelations, autocorrelograms and effective radii (Rodieck, 1991) associated to the sampled arrays were determined as described by Galli-Resta et al. (1999). While the nearest neighbour distance distribution provides a fast and easy mean to quantify array regularity, the Voronoi and Delaunay tessellations characterise the geometry of the array, or, in other words, the way an array tiles the retina. The cell Voronoi domain includes all the points in the plane closer to the cell than to any other element of the array; the Delaunay segments link each cell to those with adjacent Voronoi domains (Grumnbaum and Shephard, 1989). Autocorrelation is determined by placing one receptor at a time at the centre of the co-ordinates and replotting all the other receptors in the field with respect to this origin. This plot displays all of the possible distances between every two receptors in the field, thereby amplifying any periodicity or pattern in the relative positions of receptors. The frequency histogram of distances found in the autocorrelation, the autocorrelogram, was computed as follows. The distances represented in the autocorrelation were counted within concentric annuli. The radius increased by 5 μm moving from one annulus to the next. The counts obtained for each annulus were normalised, dividing them by the area of the annulus. These normalised counts were then plotted as a function of the annulus radius (=distance from the origin). For both cholinergic arrays, the autocorrelogram has an initial empty region, and a final plateau (Fig. 6C,G). A measure of the empty region is provided by the effective radius which is computed as follows. First, the autocorrelogram was averaged between 70 μm and 150 μm, an interval where less than 10% oscillation was observed, to obtain the average plateau value (dotted line in Fig. 6C,G). Then, the first abscissa for which the autocorrelogram reaches its plateau value is determined (arrow in Fig. 6C,G). Finally, this distance is corrected by subtracting from it the integral of the histogram between zero and this abscissa divided by the average value of the histogram at plateau (Rodieck, 1991). This correction takes into account the frequency with which neighbouring cells fall into the exclusion region.

Analysis of cell pairs

The maximal distance which identified two neighbouring array cells as a pair was defined first. Then, each sampled field containing cell pairs in the real mosaic was shifted and rotated to bring one cell of the pair in the centre of the co-ordinates, and the second cell along the positive abscissa. In this way, the positive abscissa defined the direction of the segments linking the cells of each pair, and the plots obtained for all the cell pairs could be added together to provide the average distribution of cells around cell pairs in either array. This 'total pair-autocorrelation' was then integrated within angular sectors of 45°, starting from a sector centred on the positive abscissa (the direction of the segment linking the cells of each pair), to obtain the frequency histogram of distances in different directions. Effective radii along the different directions were determined as described above. The contribution to the integration deriving from the second cell in each pair was disregarded, starting the integration in the first sector at the distance chosen as the threshold to define cell pairs.

Statistical analysis

Statistical comparisons were performed using the bootstrap analysis, to avoid assumptions about the data distribution (Efron and Tibshirani, 1991). Bootstrap is a data-based simulation method for statistical inference, which constructs a confidence interval from the real data set using a computational algorithm. Briefly, N data samples are drawn with replacement from the data set of N cases (e.g. from 1,2,3 one may extract 1,2,2). This is iterated M times (10,000 here). The amount of interest is evaluated in each case (we evaluated the histogram obtained as the difference between the corresponding normal and experimental normalised histograms), its distribution in all the bootstrap trials is obtained, and compared with that obtained

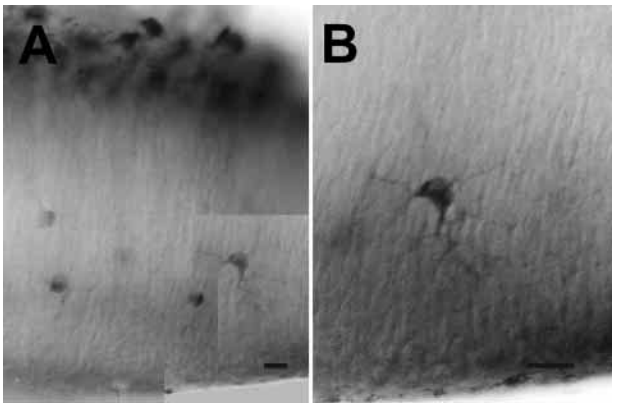

Fig. 1. The cholinergic amacrine cells express ChAT before reaching their arrays and show an initial phase of morphological differentiation. (A) Examples of ChAT cells very close to the external margin of the retina, where mitotic divisions occur. Radial section of a P0 rat retina. The montage shows ChAT cells found in 300 μm of tissue depth. (B) A number of processes develop from the cell bodies of the migrating cholinergic cells. Scale bars, 10 μm.

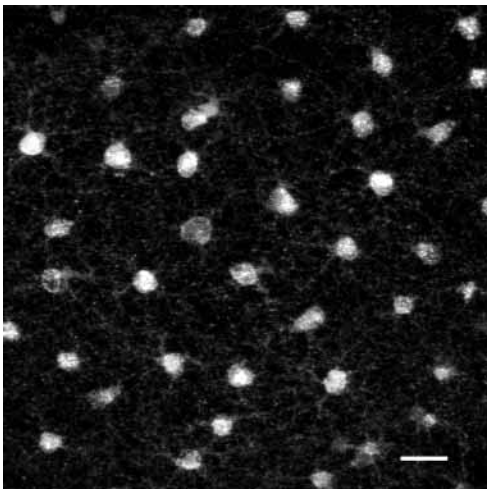

Fig. 2. Portion of the cholinergic array in the GCL layer of the P4 rat retina. ChAT immunoreactive cells are regularly spaced and linked by a fine net of dendrites in the normal GCL of the P4 rat retina. Scale bar, 20 μm.

from bootstrap comparison of separate sets of normal data. An experimental manipulation is scored as ineffective when the bootstrap estimate of the difference between the experimental and the normal histograms is lower in all bins than that obtained comparing independent normal data sets. A more detailed explanation of the bootstrap method can be found elsewhere (Efron and Tibshirani, 1991; Efron and Tibshirani, 1993). Bootstrap was performed by means of a custom made program described previously (Galli-Resta et al., 1999).

RESULTS

Cells express cholinergic markers before entering the cholinergic arrays

To investigate whether the cholinergic neurons are determined as such before entering the arrays, I have analysed the early expression of two markers unique to neurons of this type. The markers selected are the limiting rate enzyme in acetylcholine synthesis, choline acetyltransferase (ChAT), and the vesicular acetylcholine transporter (VAChT). As the cholinergic mosaics develop, cells labelled with either marker can be observed in the region that the cholinergic neurons cross to reach their layers after their genesis, as shown by the examples in Fig. 1A, B. These cells are rather sparse, e.g. in the entire region underlying the ChAT arrays a density of 16±8 cells/mm^2 is observed at birth, while the density of ChAT cells in the array is about 100 times higher. As Fig. 1B exemplifies a number of processes develop from the cell bodies of these migrating cholinergic cells. These findings suggest that before reaching their arrays the cholinergic amacrine cells express cholinergic markers and show an initial phase of morphological differentiation.

Mosaics are assembled by interactions restricted to homotypic cells

Previous computational analysis has shown that both cholinergic mosaics are statistically indistinguishable from distributions where the same number of cells have the only constraint that no two elements can be closer than a given minimal distance (Galli-Resta et al., 1997). The interactions on which these simulation are based act exclusively among mosaic elements, suggesting that the real mosaics are assembled independently of other cell types. I have tested this prediction in experimental paradigms where the relative ratio of the cholinergic cells to other cell types was altered. In a first set of experiments, the optic nerve of newborn rats was sectioned at birth (P0), causing the loss of retinal ganglion cells (RGCs) by postnatal day 2 (P2) (Perry et al., 1983). The cholinergic cells form two arrays (Fig. 2), located in two separate layers of the retina, the inner nuclear (INL) and the ganglion cell layer (GCL). After ganglion cell removal, both arrays lose one of their synaptic targets (Famiglietti, 1983). Furthermore, the cholinergic array in the GCL develops in a nearly empty layer rather than among tightly packed ganglion cells as it does in normal animals, where 90% of the cell in the GCL are ganglion cells in the first postnatal days (Rabacchi et al., 1994). New cells add to the cholinergic mosaics between P2, when all ganglion cells have disappeared, and P4 (Galli-Resta et al., 1997). On P3, the ChAT mosaics developing without ganglion cells are indistinguishable from the normal ones. Fig. 3 shows the distribution of Delaunay segments and Delaunay triangle areas (Fig. 3A,B), the distribution of nearest neighbour distances (Fig. 3C), and Voronoi domains (Fig. 3D) associated to the GCL cholinergic array in normal P3 rat retinas (line) and in P3 retinas without RGCs (squares). The distributions found in the two conditions cannot be distinguished, as confirmed by bootstrap statistical analysis, showing that the difference in the histograms obtained with of without ganglion cells are always lower than the variability found among different normal cases. These results indicate that the spatial organisation of the GCL cholinergic mosaic is independent of the tight “sea” of retinal ganglion cells among which it is normally found, and develops normally in the absence of these cells. The same results are found by analysing this mosaic at later ages (Fig. 3E-H), and apply to the INL mosaic as well (not shown). To further test the independence of the assembly of the cholinergic mosaics from other cell types, I have analysed the retina of transgenic

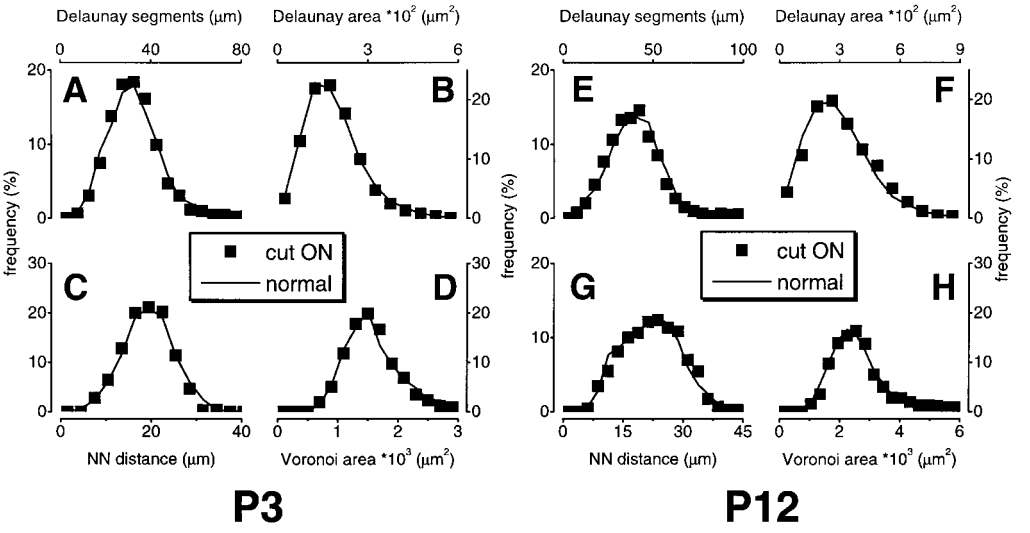

Fig. 3. The spatial organisation of the rat ChAT array in the GCL is not affected by the loss of ganglion cells. The ChAT array in the GCL has the same spatial organisation in normal rat retinas (line) and in retinas where RGCs had died following optic nerve lesion, as shown for rats aged P3 (A-D) and P12 (E-H). Array geometry was investigated by analysing the frequency distribution of the length of Delaunay segment (A,E), the areas of the Delaunay triangles (B,F), the distance between nearest neighbours (NN) (C,G) and the area of the Voronoi domains (D,H). In no case did the histogram associated to the array analysed in retinas without RGCs differ from the normal cases, as evaluated by the bootstrap method (see Methods).

mice overexpressing the antiapoptotic gene *BCL2* (Dubois-Dauphin et al., 1994) These retinas contain many more cells than normal as a consequence of the increased survival to programmed cell death induced by the transgene (Bonfanti et al., 1996; Cenni et al., 1996). The percentage of additional cells surviving death varies with cell type, thus leading to abnormal numerical ratios between different cell types. A normal number of cholinergic cells is found in the INL of the BCL2 retina (17000±1000 ChAT cells in the INL of the wild type, *n*=3; 17500±1500 BCL2, *n*=3), while their target cells, the ganglion cells are more than double their normal number (Cenni et al., 1996). Furthermore, the entire population of the INL, where this array develops, is considerably increased (Strettoi, E. personal communication). Fig. 4 illustrates the distribution of Delaunay segments and Delaunay triangle areas (Fig. 4A,B), the distribution of nearest neighbour distances (Fig. 4C) and Voronoi domains (Fig. 4D) of the INL cholinergic array found in the bcl2 transgenic retina (squares), and in the retina of wild-type mice (line). The spatial distribution of the INL cholinergic cells in the BCL2 retina is indistinguishable from what is found in the wild-type animal, independently of the greatly altered local densities of the different cell types, including the target neurons of the cholinergic amacrine cells. The identity of the spatial organisation of the INL array in the wild-type and BCL2 retina is confirmed by bootstrap analysis, showing that the difference between corresponding histograms in transgenic and wild type animals are always lower than the variability found among different wild-type cases.

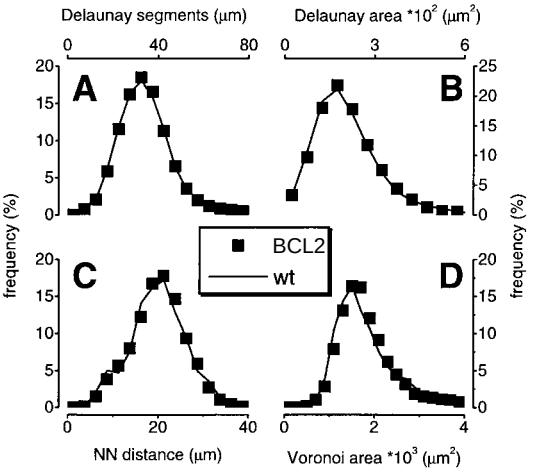

Fig. 4. The spatial organisation of the mouse ChAT array in the INL is the same in wild-type and BCL2-overexpressing mice. The array of cholinergic amacrine cells in the INL has the same spatial organisation in wild-type mouse retinas (line) and in the retinas of BCL2-overexpressing mice (squares), where the density of the cholinergic synaptic partners is greatly altered. No significant difference is observed in the frequency distribution of the length of Delaunay segment (A), the areas of the Delaunay triangles (B), the distance between nearest neighbours (C) and the area of the Voronoi domains (D), as determined by the bootstrap method (see Methods).

The interactions assembling the cholinergic arrays are non-additive and act on a short range scale

A further model prediction is that the mechanisms assembling the cholinergic mosaics are local and non-additive. According to the exclusion model the geometry of the developing cholinergic arrays can be reproduced if each array cell is able to exclude other elements from a limited surround. Since the size of this exclusion region varies from cell to cell according to a gaussian rule (Galli-Resta et al., 1997), this model can account for the rare cases of pairs of very close cells observed in the real mosaics (Fig. 5). These cells in pair however, should each 'patrol' its own exclusion domain, as they would do even without a very close neighbour. In alternative, contrary to the model prediction, pairs of very close cells could add their effects on the surrounding cells, keeping them further away that it is normally observed around single mosaic elements. This contraposition can be better illustrated by considering typical interactions of the two kinds: the physical occupancy of a domain exemplifies the first case, showing non-additive interactions, while electrical charges provide an example of additive interactions, since two neighbouring charges give rise to a stronger electrical field than a single charge.

A way to test the spatial range of the cellular "repulsive

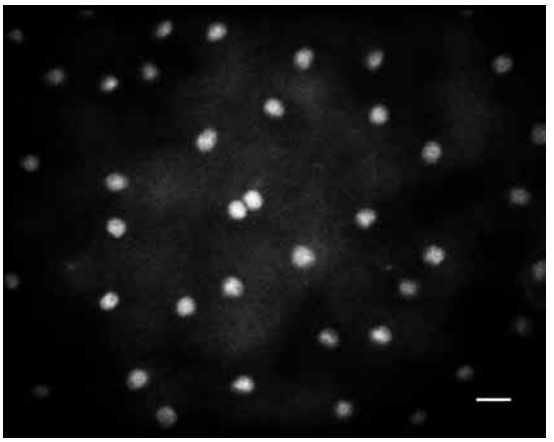

Fig. 5. Occasional pairs of cells very close to one another are found in the ChAT arrays. Portion of the cholinergic array in the INL of the P4 rat retina; Islet1 immunoreactivity is restricted to the nuclei of the cholinergic cells. Scale bar, 10 μm.

activity" is offered by the autocorrelation analysis, which plots all the distances found between any two cells in a mosaic. The autocorrelation of either cholinergic array is a nearly uniform distribution of distances, but for a central region almost devoid of other ChAT cells, as shown by the examples in Fig. 6A,E. This nearly empty zone is the "exclusion region" that each cell keeps clear of other cells of the same type. Similar plots can be computed to analyse how cells are distributed around the occasional pairs of very close cells found in the mosaics. If the exclusion mechanisms are non-additive, a third mosaic cell should only feel the effect of the cell in the pair to which it is closer. Plotting cell positioning around cell pairs, one should expect an oblong exclusion region, obtained by placing one next to the other the circular exclusion regions associated with either cell of the pair. If the interactions are additive, on the other hand, the exclusion domain associated with a pair of cells should be larger in all directions than that associated with a single cell, in the same way as the electrical field generated by two charges is stronger than the field generated by either alone, or the local concentration of diffusible substances is higher around two neighbouring sources than close to a single one.

Autocorrelation analysis has been performed in the rat retina on P4, the earliest age at which the cholinergic mosaics are complete (Galli-Resta et al., 1997). This choice avoids the potential distortion induced by the subsequent anisotropic retinal growth (McCall et al., 1987). Considering that the cell soma is about 8 μm in diameter (e.g. Fig. 2), and the average spacing between neighboring cells in the arrays is around 35 μm (average Delaunay segment in Fig. 3A), I have arbitrarily defined as pairs cells which are within 10 μm of one another. About 2% of the cells lay within 10 μm of their closest neighbour in the GCL cholinergic mosaic (124 in 5792 sampled cells), and 2.5% in the INL mosaic (191 in 7643 cells). In a second analysis I have chosen a 12.5 μm threshold to study a larger sample of cell pairs (5% of the cells in the GCL array, 8% in the INL array). Having defined cell pairs, each field containing a cell pair was replotted in a new set of co-ordinates where one cell of the pair was in the origin, and the second cell was along the positive abscissa. In this way, all the plots obtained for either array could be added together, to provide the average distribution of cells around cell pairs. The results obtained for pairs of cells found within 12.5 μm of one another are shown in Fig. 6B for the INL array, and in Fig. 6F for the GCL array. The main difference with respect to the autocorrelation computed for single cells (Fig. 6A,E) is that the central empty domain surrounding cell pairs is an oblong region, which appears larger than the region associated with single cells only along the positive abscissa, which is the direction of the segments joining the two cells of each pair. To facilitate the comparison, a large black dot indicates the centre of the co-ordinates in Fig. 6A,B,E,F.

To quantify the size of the exclusion regions, the frequency histograms of distances (autocorrelograms) were derived from the autocorrelations. Examples are in Fig. 6C,G. The autocorrelograms show that the distance between any two cells in either array is never below 8 μm (the average diameter of the cell body, e.g. Fig. 2), it is rarely below 15-20 μm, rises to a local peak, and gradually reaches an equal probability of being any length beyond 40 μm in the INL, 60 μm in the GCL. While the initial region of lower probability is intuitively associated with an exclusion rule, the small peak preceding the plateau may seem surprising. However, this peak is predicted by the exclusion model, and reflects the density of cells in the array. If each cell excludes other cells from a limited domain, and a lot of cells do the same in the layer, then any new cell will be placed where an additional exclusion domain can fit. As the density of cells increases, this is reflected by a higher probability of cell positioning right outside the exclusion regions of other cells (Galli-Resta et al., 1999). The essential feature of the autocorrelogram is thus the initial region of low probability. A measure of this exclusion region is the effective radius (Rodieck, 1991), which is the abscissa where the autocorrelogram first reaches its plateau value (arrows in Fig. 6C,G), minus a small correction taking into account the percentage of cells falling into the exclusion region (see Methods). The average effective radius is 16.3±1.8 μm (mean±standard deviation) for the GCL mosaic, and 13.7±1.7 μm for the INL array. Effective radii can also be derived from the autocorrelation restricted to cell pairs (Fig. 6B,F), provided separate autocorrelograms are computed in different directions, to distinguish the exclusion effects in different locations around the cell pair. Here the autocorrelation was integrated in 8 contiguous angular sectors of 45°. The "effective radii" obtained around cell pairs are shown in Fig. 6D,H (squares), together with the measure obtained for single cells (gray contour), and the schematic localisation of the two cells of the pairs, represented by open circles. The same results are obtained considering 10 μm or 12.5 μm as the threshold distance to define cell pairs. These graphs clearly show that the effects of cells in pairs are just what one would obtain by aligning the two exclusion regions associated to either cell of the pair. No enlargement of the exclusion domain is observed perpendicular to the cell pair, nor along the negative abscissa (the origin is defined by the leftmost cell of the pair). Simply, the exclusion domain is larger along the positive abscissa, where the second cell of the pair keeps cells away from its own exclusion domain, as any other mosaic cells does. In other words, the effects of a pair of cells are in each point those of the cell closest to that point, with no additional contribution by the other cell of the pair. This indicates non-additive interactions.

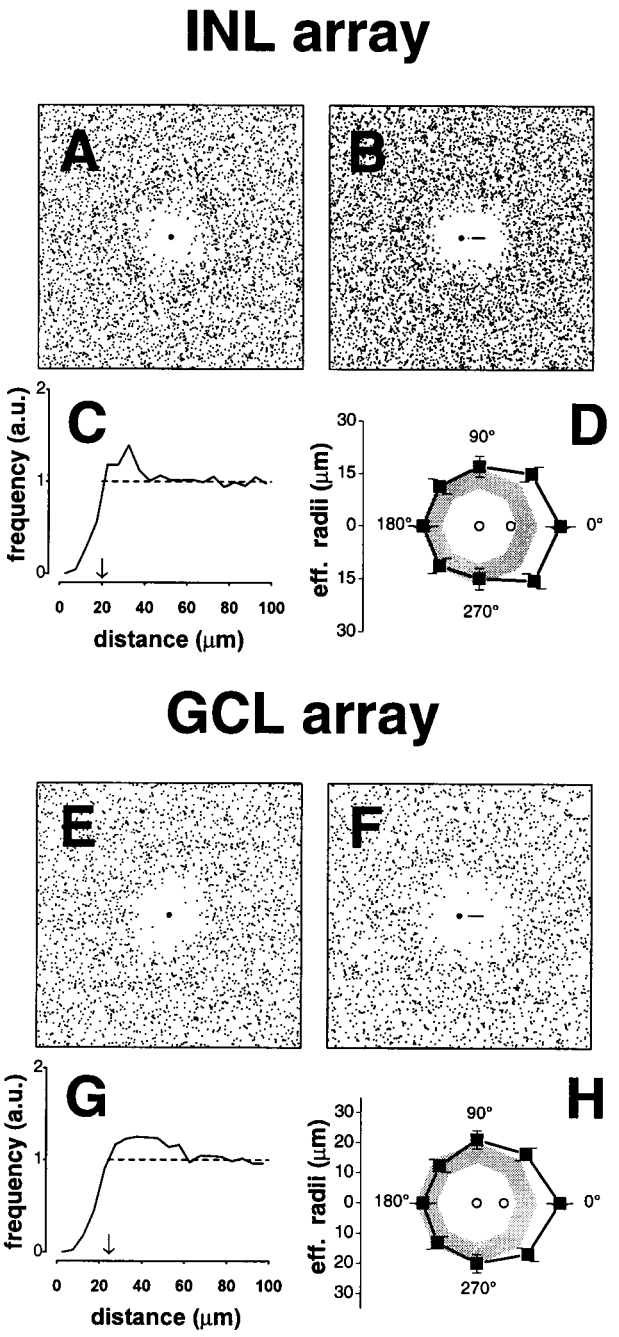

Fig. 6. The interactions controlling array assembly are non-additive and short ranged. This analysis compares the positions of mosaic cells around single mosaic elements (autocorrelation in A, E) and around cell pairs (B,F). Cell pairs are here defined arbitrarily as cells lying within 12.5 μm of one another. (A,E) The autocorrelation of either cholinergic array is a uniform distribution of distances, but for a central empty region, which is the area devoid of other ChAT cells that surround any mosaic element. Typical examples are illustrated in A for the INL array, in E for the GCL array. The large dots represent the origin. (B,F) Similar plots can be computed, representing the distribution of cells around cell pairs, as shown in B for the INL array, in F for the GCL array. One cell of each pair is in the centre of the co-ordinates (large dot), the second cell is along the positive abscissa (dots along the positive abscissa within the central empty area). These plots have a central oblong empty region, which appears larger than the region associated to single cells only along the positive abscissa, that is the direction of the segments joining the two cells of each pair. (C,G) Examples of autocorrelograms for the INL array (C), and for the GCL array (D). These histograms show that the distance between any two cells in either array is never below 8 μm (the cell size, e.g. Fig. 2), it is rarely below 15-20 μm, rises to a local peak, and gradually reaches an equal probability of being any length beyond 40 μm in the INL, 60 μm in the GCL (the plateau level is indicated by the horizontal dotted line). A measure of the exclusion region, the effective radius, is derived from this histogram as described in the text. Effective radii have also been derived from the autocorrelation restricted to cell pairs (B,F), computing the autocorrelograms separately in different directions, to distinguish the exclusion effects in different positions around the cell pair. The "effective radii' obtained around cell pairs are shown in (D,H) as squares, together with the measure obtained for single cells (gray contour), and the schematic representation of the two cells of the pair (open circles). These graphs show that the effects of cells in pairs are just what one would obtain by aligning the two exclusion regions associated to either cell of the pair. No enlargement of the exclusion domain is observed perpendicular to the cell pair, nor along the negative abscissa (the origin is defined by the leftmost cell of the pair). Simply, the exclusion domain is larger along the positive abscissa, where the second cell of the pair keeps cells away from its own exclusion domain, as any other mosaic cell does. The effects of a pair of cells are, at each point, those of the cell closest to that point, as in the case of non-additive interactions. This analysis was performed on P4 rat retina. The data illustrated refer to pairs defined as cells within 12.5 μm of one another, but the same results are obtained considering 10 μm as the threshold distance to define cell pairs.

This analysis also defines the spatial range of the interactions controlling cell spacing in the cholinergic mosaics. The autocorrelation indicates that each mosaic cell affects the probability of other cell positioning only in a limited region surrounding it. Indeed, as shown by Fig. 6C,G, beyond 40-60 μm the autocorrelation is flat, indicating that the probability that other mosaic cells are placed beyond this limit becomes independent of the cell in the origin. Thus, the effective "repulsive action" exerted by each mosaic cell is of relatively short range, acting over a distance corresponding to a few cell body diameters.

DISCUSSION

Combining experimental and computational techniques four properties of the mechanisms controlling cell positioning in the retinal cholinergic arrays have been defined. The cholinergic fate is determined before cells enter the arrays and the regular cell spacing in either array derives from local interactions, which are non-additive, and involve exclusively cells of the same type.

A first set of experiments has shown that markers unique to the cholinergic amacrine cells in the retina, choline acetyltransferase (ChAT) and the vesicular acetylcholine transporter (VAChT), are expressed by neurons which are found along the migratory pathway that newborn cells must cross to reach their layers. ChAT is the rate limiting enzyme in the synthesis of acetylcholine, which, in the retina, is a transmitter unique to the cholinergic amacrine cells (Masland and Tauchi, 1986). VAChT is the vesicular transporter for acetylcholine, responsible for the concentration of this transmitter within synaptic vesicles (Usdin et al., 1995). These results strongly suggest that the cholinergic neurons are determined as such before migrating to their final destination.

This clarifies the issue that the identification of migratory neurons by means of Islet-1 expression had left open, since these neurons could have been ganglion cells or cholinergic amacrine cells which both express this transcription factor (Galli-Resta et al., 1997).

A second set of experiments has shown that the positional constraints that assemble regular arrays of cholinergic neurons are independent of other cell types. This has been verified by manipulations altering the number of target cells and the cellular density in the layers where the cholinergic arrays develop. The cholinergic cells have no regular spacing while migrating, but appear ordered once in their layers, and actively maintain their spacing as new cells enter the arrays in the first postnatal days (Galli-Resta et al., 1997). This suggests that it is only once these cells are in their layers, and not at earlier times, that patterning interactions occur. Therefore, I have focused on manipulations altering the retina at times when the cholinergic arrays are actively forming in their layers, and not at earlier times. No attempt was made to alter the cells providing input to the cholinergic amacrine cells, since the ChAT mosaics develop when bipolar cells are still absent (Cepko, 1993), suggesting that the assembly of the cholinergic mosaics is independent of the bipolar cells. In the retinas of BCL2 overexpressing mice, the INL cholinergic array has a normal number of cells. The correct number of elements appears sufficient to allow the development of a normal mosaic, notwithstanding the aberrant environment, where the density of target cells is double than normal (Cenni et al., 1996), and many more cells are found in the layer where the mosaic develops (Strettoi E. personal communication). Similarly, the GCL cholinergic mosaic has the same spatial organisation in rat retinas whether ganglion cells are present or absent following optic nerve section at birth. Considering that 90% of the cells in the GCL are ganglion cells in the first postnatal days (Rabacchi et al., 1994), one can conclude that the GCL cholinergic mosaic develops in the same way in the almost empty ganglion cell layer, or surrounded by the densely packed ganglion cells in the normally developing retina. This independence is observed already on P3, when the mosaic is still developing and actively maintains its organisation while new cells add to it (Galli-Resta et al., 1997), suggesting that even the dynamics of mosaic development is independent of the presence of cells of other types (including target cells) in the same layer.

A different analysis has focused on the additivity and the spatial range of the interactions controlling cell positioning in the cholinergic mosaics. The occasional presence of cells very close to one another in the real mosaics allows the investigation of whether two close-by cells add their effects on the surrounding mosaic elements. Simulations based on an exclusion rule (Galli-Resta et al., 1997) do not predict interaction additivity. This was verified directly by comparing the positioning of mosaic cells around cell pairs and around single mosaic elements, as the autocorrelation allows to do. This analysis shows that each mosaic cell “patrols” a limited surround, where the probability of finding other mosaic cells is significantly low (the exclusion region). When two cells are very close to one another, the autocorrelation is just what one would obtain by aligning the two exclusion regions associated with the cells of the pair. Either cell in a pair appears to patrol just its own exclusion domain, and the effects in each location are those of the cell of the pair which is closer to that location. This indicates non-additive interactions. The same analysis has shown also that each mosaic element affects the probability of other cells positioning only in the range of a few cell diameters. Beyond such limit the autocorrelation is flat, indicating that the probability of cell positioning becomes independent of the cell in the origin.

This paper does not describe molecular players or cellular processes involved in mosaic assembly, yet it defines some of their properties, characterising the spatial range of the interactions controlling mosaic formation, their lack of additivity, and their restriction to array cells. In light of the present data, diffusible factors (here intended in a broad sense spanning from passive diffusion to spreading by relay mechanisms) seem unlikely candidates for controlling mosaic assembly, since additivity in the case of close-by sources (two sources=double effect) would not escape the autocorrelation test. An exception is represented by the paradigm of two competing diffusible signals, one causing the cell response, the second limiting the spatial range of the former (Meinhardt, 1992; Freeman, 1997). Although additive, this modality of interaction may define such sharp boundaries to the region where the effects of a single cell are felt, that even when very close, two cells would affect only a small additional region beyond their normal areas of influence, and this may remain hidden within the experimental error. With the former exception, molecules should be considered that mediate non-additive interactions of the sort of contact inhibition, which is exactly what exclusion models simulate.

Although restricted, the region from which each cholinergic cell excludes other mosaic cells exceeds the size of the cell soma. Yet, this analysis calls for highly localised, possibly contact-mediated signalling to account for the regular cell spacing of the cholinergic cells. This suggests the involvement of the continuous net of dendrites that the cells of either array develop while their mosaics are forming (e.g. Fig. 2; Galli-Resta, unpublished data). Local repulsive or inhibitory interactions between dendrites could define the territory where the cell dendritic tree or its central core can develop. The radial symmetry of the cholinergic amacrine cells, which has gained them the name of “starburst cells” (Masland and Tauchi, 1986), suggests that constraints on dendritic positioning could suffice to define the position of the cell body, leading to the regular cell spacing observed in the cholinergic arrays.

This study is focused on the cholinergic amacrine cells which form two well characterised mosaics early in development (Galli-Resta et al., 1997), and play a pivotal role in the propagation of waves of spontaneous activity that allows the eye-specific segregation of retinal projections in the brain (Feller et al., 1996; Penn et al., 1998). The present findings, considered alongside our previous results (Galli-Resta et al., 1997), clarify the sequence of events in the assembly of the cholinergic arrays. Cells become cholinergic before entering the arrays, when they still have no minimal spacing (Galli-Resta et al., 1997 and unpublished). Within the mosaic layers, unknown mechanisms allow the interactions and recognition between cholinergic cells. These interactions lead mosaic cells to take appropriate distances from one another, and to actively maintain this regular spacing as new cells join the array (Galli-Resta et al., 1997). This occurs by means, at least, of relative movement (Reese et al., 1995; Galli-Resta et al., 1997; Reese and Tan, 1998), which is observed at these times (Reese et al., 1999), and possibly via cell death (Cook and Chalupa, 2000). The processes controlling cell

positioning resemble the physical clearance of a domain surrounding each mosaic element (Galli-Resta et al., 1997). The constancy of this domain (Galli-Resta et al., 1997; Galli-Resta, 1998), and its dependence exclusively on homotypic interactions suggest that it derives from cell intrinsic properties which characterise the differentiated or developing cholinergic cells, like for example the average size of the dendritic tree during development or that of its central core.

An important open question is whether the cell-type "autonomy" of mosaic assembly applies to other retinal mosaics, as suggested by the general good fit of exclusion rules (Scheibe et al., 1995; Galli-Resta et al., 1997; Galli-Resta et al., 1999), and by the almost general lack of spatial correlation between mosaics formed by neurons of different types (Rockhill et al., 2000). If retinal mosaics develop independently of one another, one could envision an economical and powerful plan to pattern the retina on the basis of local rules. Retinal arrays are laid down by homotypic interactions early in development, then recognition and interactions between appropriate synaptic partners within a limited spatial range are sufficient to lay down a modular architecture with topographically ordered connections. Additional adjustments could then take place to further refine this modular circuitry and to create specialized features like the fovea (Hendrikson, 1994).

I thank G. Resta for computer programming, E. Novelli for technical assistance, E. Strettoi for providing me with the mouse retinas, J.-C. Martinou for the BCL2 transgenic mice, E. Putignano for PCR analysis of the BCL2 mouse tissue, A. Fiorentini, L. Maffei, F. Rossi and M. C. Morrone for helpful comments on the manuscript. This work was supported by the CNR and the European Commission, DGXII, Biotech Program.

REFERENCES

Bonfanti, L., Strettoi, E., Chierzi, S., Cenni, M., Liu, X., Martinou, J.-C., Maffei, L. and Rabacchi, S. (1996). Protection of retinal ganglion cells from natural and axotomy-induced cell death in neonatal transgenic mice overexpressing bcl-2. *J. Neurosci.* **16**, 4186-4194.

Bumsted, K., Jasoni, C., Szel, A. and Hendrickson, A. (1997). Spatial and temporal expression of cone opsins during monkey retinal development. *J. Comp. Neurol.* **378**, 117-134.

Cenni, M., Bonfanti, L., Martinou, J.-C., Ratto, G., Strettoi, E. and Maffei, L. (1996). Long-term survival of retinal ganglion cells following optic nerve section in adult *BCL2* transgenic mice. *Eur. J. Neurosci.* **8**, 1735-1745.

Cepko, C. L. (1993). Retinal cell fate determination. In *Progress in Retinal Research* Vol. 12 (ed. N. Osborn and R. Chader), pp. 1-12. Oxford: Pergamon Press.

Cepko, C. L. (1996). The patterning and onset of opsin expression in vertebrate retinae. *Curr. Opin. Neurobiol.* **6**, 542-546.

Cook, J. E. and Chalupa, L. M. (2000). Retinal mosaics: new insights into an old concept. *Trends Neurosci.* **23**, 26-34.

Dowling, J. E. (1987). *The Retina, an Approachable Part of the Brain.* Cambridge, MA: Harvad University Press.

Dubois-Dauphin, M., Frankowski, H., Tsujimoto, Y., Huarte, J. and Martinou, J.-C. (1994). Neonatal motoneurons over-expressing the bcl-2 protooncogene in transgenic mice are protected from axotomy induced cell death. *Proc. Natl. Acad. Sci. USA* **94**, 3309-3313.

Efron, B. and Tibshirani, R. J. (1991). Statistical data analysis in the computer age. *Science* **253**, 390-395.

Efron, B. and Tibshirani, R. J. (1993). *An Introduction to the Bootstrap*. New York: Chapamn and Hall.

Famiglietti, E. J. (1983). On and off pathways through amacrine cells in mammalian retina: the synaptic connections of "starburst" amacrine cells. *Vision Res.* **23**, 1265-1279.

Feller, M. B., Wellis, D. P., Stellwagen, D., Werblin, F. S. and Shatz, C. J. (1996). Requirement for cholinergic synaptic transmission in the propagation of spontaneous retinal waves. *Science* **272**, 1182-1187.

Freeman, M. (1997). Cell determination strategies in the *Drosophila* eye. *Development* **124**, 261-270.

Galli-Resta, L. (1998). Patterning the vertebrate retina: the early assembly of retinal mosaics. *Seminars Cell Dev. Biol.* **9**, 279-284.

Galli-Resta, L. and Ensini, M. (1996). An intrinsic limit between genesis and death of individual neurons in the developing retinal ganglion cell layer. *J. Neurosci.* **16**, 2318-2324.

Galli-Resta, L., Novelli, E., Kryger, Z., Jacobs, G. and Reese, B. (1999). Modelling the mosaic organization of rod and cone photoreceptors with a minimal spacing rule. *Eur. J. Neurosci.* **11**, 1438-1446.

Galli-Resta, L., Resta, G., Tan, S.-S. and Reese, B. (1997). Mosaics of Islet-1 expressing amacrine cells assembled by short range cellular interactions. *J. Neurosci.* **17**, 7831-7838.

Grumnbaum, B. and Shephard, G. C. (1989). Tilings and Patterns. An introduction. New York, NY, USA: Freeman and Co.

Hendrikson, A. E. (1994). Primate foveal development: a microcosm of current questions in neurobiology. *Invest. Oph. Vis. Sci.* **35**, 3129-3133

Larison, K. D. and Bremiller, R. (1990). Early onset of phenotype and cell patterning in the embryonic zebrafish retina. *Development* **109**, 567-576.

MacNeil, M. and Masland, R. (1998). Extreme diversity among amacrine cells: implications for function. *Neuron* **20**, 971-982.

Masland, R. H. (1996). Processing and encoding of visual information in the retina. *Curr. Opin. Neurobiol.* **6**, 467-474.

Masland, R. H. and Tauchi, M. (1986). The cholinergic amacrine cell. *Trends Neurosci* **9**, 218-223.

McCall, M., Robinson, S. and Dreher, B. (1987). Differential retinal growth appears to be the primary factor producing the ganglion cell density gradient in the rat. *Neurosci. Letts.* **79**, 78-84.

Meinhardt, H. (1992). Pattern-formation in biology – a comparison of models and experiments. *Reports on Progress in Physics* **55**.

Penn, A. A., Riquelme, P. A., Feller, M. B. and Shatz, C. J. (1998). Competition in retinogeniculate patterning driven by spontaneous activity. *Science* **279**, 2108-2112.

Perry, V. H., Henderson, Z. and Linden, R. (1983). Postnatal changes in retinal ganglion and optic axon populations in the pigmented rat. *J. Comp. Neurol.* **219**, 356-368.

Rabacchi, S. A., Ensini, M., Bonfanti, L., Gravina, A. and Maffei, L. (1994). Nerve growth factor reduces apoptosis of axotomized retinal ganglion cells in the neonatal rat. *Neurosci.* **63**, 969-973.

Raymond, P. A., Barthel, L. K. and Curran, G. A. (1995). Developmental patterning of rod and cone photoreceptors in embryonic zebrafish. *J. Comp. Neurol.* **359**, 537-550.

Reese, B., Necessary, B., Tam, P., Faulkner-Jones, B. and Tan, S. (1999). Clonal expansion and cell dispersion in the developing mouse retina. *Eur. J. Neurosci.* **11**, 2965-2978.

Reese, B. E., Harvey, A. R. and Tan, S.-S. (1995). Radial and tangential dispersion patterns in the mouse retina are cell-class specific. *Proc. Natl. Acad. Sci. USA* **92**, 2494-2498.

Reese, B. E. and Tan, S.-S. (1998). Clonal boundary analysis in the developing retina using X-inactivation transgenic mosaic mice. *Semin. Cell Dev. Biol.* **9**, 285-292.

Rockhill, R. L., Euler, T. and Masland, R. H. (2000). Spatial order within, but not between types of retinal neurons. *Proc. Natl. Acad. Sci. USA* (in press).

Rodieck, R. W. (1991). The density recovery profile: a method for the analysis of points in the plane applicable to retinal studies. *Vis. Neurosci.* **6**, 95-111.

Rodieck, R. W. (1998). *The First Steps in Seeing*. Suterland, MA: Sinauer Associated.

Scheibe, R., Schnitzer, J., Röhrenbeck, J., Wohlrab, F. and Reichenbach, A. (1995). Development of A-type (axonless) horizontal cells in the rabbit retina. *J. Comp. Neurol.* **354**, 438-458.

Usdin, T., Eiden, L., Bonner, T. and Erickson, J. (1995). Molecular biology of the vesicular ACh transporter. *Trends Neurosci.* **18**, 218-224.

Wässle, H. and Boycott, B. B. (1991). Functional architecture of the mammalian retina. *Physiol. Rev.* **71**, 447-480.

Wässle, H. and Riemann, H. J. (1978). The mosaic of nerve cells in the mammalian retina. *Proc. Royal Soc. London B* **200**, 441-461.

Wikler, K. C. and Rakic, P. (1991). Relation of an array of early-differentiated cones to the photoreceptor mosaic in the primate retina. *Nature* **351**, 397-400.

Wikler, K. C., Rakic, P., Bhattacharyya, N. and Macleish, P. R. (1997). Early emergence of photoreceptor mosaicism in the primate retina revealed by a novel cone-specific monoclonal antibody. *J. Comp. Neurol.* **377**, 500-508.